International Journal of Automotive Technology, Vol. 7, No. 5, pp. 535–545 (2006)

1229-9138/2006/029-03

NONLINEAR ANALYSIS OF SELF-EXCITED VIBRATION IN WHEELED TRACTOR VEHICLE'S DRIVELINE

X.-H. LI*, J.-W. ZHANG and C.-C. ZENG

National Key Laboratory of Vibration, Shock and Noise, School of Mechanical Engineering, Shanghai Jiaotong University, Shanghai 200030, China

(Received 6 July 2005; Revised 15 March 2006)

ABSTRACT–A nonlinear analysis of torsional self-excited vibration in the driveline system for wheeled towing tractors was presented, with a 2-DOF mathematical model. The vibration system was described as a second-order ordinary differential equation. An analytical approach was proposed to the solution of the second-order ODE. The mathematical neighborhood concept was used to construct the interior boundary and the exterior boundary. The ODE was proved to have a limit cycle by using Poincaré-Bendixson Annulus Theorem when two inequalities were satisfied. Because the two inequalities are easily satisfied, the self-excited vibration is inevitable and even the initial slip rate is little. However, the amplitude will be almost zero when the third inequality is satisfied. Only in a few working modes of the towing tractor the third inequality is not satisfied. It is shown by experiments that the torsional self-excited vibration in the driveline of the vehicle is obvious.

KEY WORDS : Self-excited vibration, Towing tractor, Driveline

1. INTRODUCTION

Because severe vibrations of the driveline system of a vehicle have great influence on driving performance, a theoretical analysis of the dynamic behaviors is of very significance for automotive engineers in the design of the driveline system (Hwang *et al.*, 2000). The self-excited vibrations of the clutch and the gear rattle were studied by by Zhu and Parker (Farong and Parker, 2005), Couderc, Callenaere and Hagopian (Couderc *et al.*, 1998), Hwang, Joseph and Ling (Hwang *et al.*, 1998), and Christopher and Shan (Christopher *et al.*, 1992). However, few of them discussed the varying longitudinal adhesive forces on dynamic behaviors of the vehicle. In 1960's, jumping phenomenon was found when wheeled tractor was towing a heavy trailer. In their experiments by Bailey, Reece and Wills (Bailey *et al.*, 1962), jumping phenomenon happened when the slip rate was bigger than 30%, and traction was found to be vibrating. By experiments, previous researchers (Ford and Karam, 1991; Jia *et al.*, 1996; Zheng *et al.*, 1996; Jia *et al.*, 1997a; 1997b; Zheng *et al.*, 1997; Jia *et al.*, 1998; Wang, 2000; Zheng *et al.*, 2001; Ge *et al.*, 2003) pointed out the torsional vibration in the driveline is a kind of self-excited vibration. As a result of their experiments, they pointed out that there was self-excited vibration only when the slip rate was large enough. However, their research would be more reasonable if they had considered the longitudinal velocity of the tractor is not a constant when there is the existence of the self-excited vibration. In mathematics, a limit circle of a differential equation means the self-excited vibration in the vibration system. However, none of the previous researchers proved the self-excited vibration in the driveline by mathematical analysis, and they didn't answer why there is no self-excited vibration while the initial slip rate is little.

In this paper, a nonlinear analysis of self-excited vibration in the driveline for wheeled tractor vehicle was presented with mathematic proof. Firstly, a 2-DOF vibration system of the driveline was built. The towing working mode, in which the opening angle of the diesel engine's throttle valve is a constant, was considered, and the angular velocity of the diesel engine was considered as a slowly varying function. The system of the tractor vehicle and the trailer was also considered. Then, the 2-DOF vibration system was described as a second-order ordinary differential equation (ODE), and Poincar-Bendixson Annulus Theorem was used to prove that there must exist a limit circle when two inequalities were satisfied. Then, the amplitude of the self-excited vibrations was proved to be almost zero when a third inequality was satisfied. At last, Experiments show the existence of the torsional self-excited vibration in wheeled tractor vehicle's driveline.

*Corresponding author. e-mail: lixianghua@china.com.cn

2. MODELING

2.1. Torsional Vibration System of Tractor's Driveline

The driveline of a rear-wheel-drive tractor vehicle can be simplified as a torsional vibration system. The engine and the flywheel are united as one cell, and modeled as an inertial component. Driving wheels are united as one cell, and modeled as another inertial component. The other parts of the driveline are supposed to be torsional spring and damper. This simplified vibration system is shown as Figure 1.

While θ_w and θ_e define the rotations of the tractor's driving wheel and the engine, the equations of motion for the driving wheel and the engine are given by

$$J_w\ddot{\theta}_w = -K(\theta_w - \theta_e) - C(\dot{\theta}_w - \dot{\theta}_e) - F_{1Z}R_w\mu(s) + F_{1Z}f_1R_w \quad (1)$$

$$J_e\ddot{\theta}_e = T_e - K(\theta_e - \theta_w) - C(\dot{\theta}_e - \dot{\theta}_w). \quad (2)$$

where

J_e equivalent rotary inertia of the tractor's engine and flywheel
J_w driving wheels' equivalent rotary inertia
$\mu(s)$ adhesive coefficient
s slip
T_e tractor's engine torque
K torsional stiffness of the tractor's driveline
C torsional damping of the tractor's driveline
R_w effective rolling radius of the driving wheel
F_{1Z} vertical loading on the tractor's driving wheels
m_1 mass of the tractor
f_1 tractor's coefficient of rolling resistance.

In the case of the tractor towing a trailer (See Figure 2), F_{1Z} can be expressed as follows

$$F_{1Z} = \frac{m_1 g L_f}{L_r + L_f}\cos(\alpha) \quad (3)$$

where

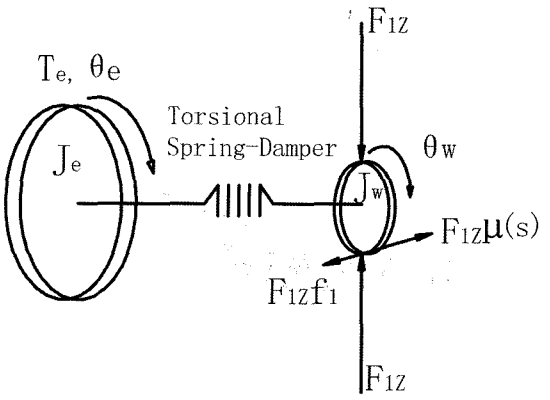

Figure 1. The dynamic model of the torsional vibration system.

α slope of the road
L_f distance between front axle and the tractor's center of gravity
L_r distance between rear axle and the tractor's center of gravity

The tractor vehicle and the trailer are pulled ahead by the longitudinal friction forces on the driving wheels of the tractor vehicle, and the longitudinal friction forces are related to the adhesion coefficient and the vertical loading acting on the wheels. The longitudinal friction force is dependent principally on the adhesive coefficient $\mu(s)$ and the vertical loading. The adhesive coefficient $\mu(s)$ is expressible with respected to the slip s of the following form as (Olson *et al.*, 2000).

$$\mu(s) = c_1[1 - \exp(-c_2 s)] - c_3 s \quad (4)$$

where c_1, c_2 and c_3 are road constant parameters, which are determined according to the tractor tire-road interaction. For convenience, however, the slip s may be presented according to the definition as

$$s = 1 - \frac{u}{\dot{\theta}_w R_w} \quad (5)$$

where u is the tractor's longitudinal velocity.

As shown in Figure 2, the equation of motion for the system of the tractor and the trailer is given by

$$(m_1+m_2)\dot{u} = F_{1Z}\mu(s) - m_1 g\cos(\alpha)f_1 - m_2 g\cos(\alpha) f_2 - (m_1 + m_2)g\sin(\alpha) \quad (6)$$

where

m_2 mass of the trailer
f_2 trailer's coefficient of rolling resistance

Addition of Equation (1), Equation (2) and Equation (6) multiplied with R_w yields

$$(m_1 + m_2)R_w\dot{u} + J_w\ddot{\theta}_w + J_e\ddot{\theta}_e = T_e - \left[\frac{L_r}{L_r + L_f}m_1 g\cos(\alpha)f_1 + m_2 g\cos(\alpha)f_2 + (m_1+m_2)g\sin(\alpha)\right]R_w \quad (7)$$

Although the diesel engine torque is a function of many parameters, it is assumed here that the engine torque is determined only by the opening angle of the throttle valve. This means that the engine torque is kept

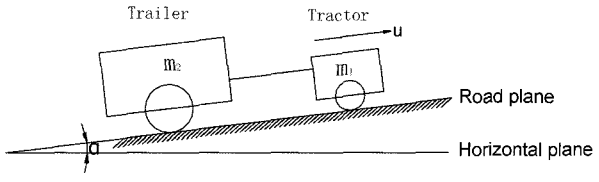

Figure 2. The sketch of the tractor and the trailer.

constant while the opening angle of the throttle valve holds unchanged. When the tractor towing a trailer is driven on a hillside road with a constant slope, and the opening angle of the throttle valve remains constant, if the engine torque satisfies the equation as follows

$$T_e=\left[\frac{L_r}{L_r+L_f}m_1 g\cos(\alpha)f_1+m_2 g\cos(\alpha)f_2+(m_1+m_2)g\sin(\alpha)\right]R_w \tag{8}$$

then, substituting Equation (8) into Equation (7) and then integration yield

$$\begin{aligned}&(m_1+m_2)R_w u+J_w\dot{\theta}_w+J_e\dot{\theta}_e=\\&(m_1+m_2)R_w^2(1-s_0)\omega_{w0}+J_w\omega_{w0}+J_e\omega_{e0}\end{aligned} \tag{9}$$

where s_0, ω_{w0} and ω_{e0} are respectively the initial values of s, $\dot{\theta}_w$ and $\dot{\theta}_e$, and the initial values here mean the values respected to the beginning of being constant opening angle of the throttle valve. Substituting Equation (9) into Equation (5) yields

$$s=b_0-b_{10}\frac{\omega_{w0}}{\dot{\theta}_w} \tag{10}$$

where

$$b_0=1+\frac{J_w}{(m_1+m_2)R_w^2}$$

$$b_{10}=\frac{(m_1+m_2)R_w^2(1-s_0)+J_w+(J_e\omega_{e0}-J_e\theta_e)/\omega_{w0}}{(m_1+m_2)R_w^2} \tag{11}$$

By the variable transformation of

$x=\dfrac{\dfrac{c_1-c_3b_0-f_1}{J_w}F_{1Z}R_w+\dfrac{T_e}{J_e}}{\left(\dfrac{1}{J_w}+\dfrac{1}{J_e}\right)K}+\theta_w-\theta_e$, and from Equation (1), Equation (2), Equation (3), Equation (4) and Equation (10), we have two equations as follows

$$\ddot{x}+a_0x+a_1\dot{x}-a_2e^{c_2b_{10}\frac{\omega_{w0}}{\dot{x}+\dot{\theta}_e}}+a_3b_{10}\frac{\omega_{w0}}{\dot{x}+\dot{\theta}_e}=0 \tag{12}$$

and

$$J_e\ddot{\theta}_e=T_e+Kx+C\dot{x}-\frac{\dfrac{c_1-c_3b_0-f_1}{J_w}F_{1Z}R_w+\dfrac{T_e}{J_e}}{\left(\dfrac{1}{J_w}+\dfrac{1}{J_e}\right)} \tag{13}$$

where

$$a_0=\left(\frac{1}{J_w}+\frac{1}{J_e}\right)K$$

$$a_1=\left(\frac{1}{J_w}+\frac{1}{J_e}\right)C$$

$$a_2=\frac{m_1gL_f\cos(\alpha)R_wc_1}{\left(L_f+L_r\right)J_we^{c_2b_0}}$$

$$a_3=\frac{m_1gL_f\cos(\alpha)R_wc_3}{J_w\left(L_f+L_r\right)}$$

By Equation (12) and Equation (13) the dynamic behaviors of the 3D vibration system are described in terms of x, $\dot{x}$ and $\dot{\theta}_e$. Thus, the 3rd order ordinary differential equation may be derived out theoretically by elimination of the associated Equations (12) and (13). However, to a 3-order ODE, whether it has a limit circle is still a challenge in mathematics, and this 3-order differential equation is difficult to analysis its trajectory.

2.2. Simplified 2-Dimension Model

The diesel engine's angular velocity $\dot{\theta}_e$ is a slowly varying function while the opening angle of the throttle valve is a constant. And this slowly varying function $\dot{\theta}_e$ can be expressed as follows:

$$\dot{\theta}_e=\omega_{eT}+h_0\tilde{t} \tag{14}$$

where $\tilde{t}=\varepsilon t$ is the slow scale, $0<\varepsilon\square 1$, $0<h_0\square\omega_{eT}$, and ω_{eT} is the mean value of $\dot{\theta}_e$ during the time in which the opening angle of the throttle valve is a constant. Insertion of Equation (14) to Equation (11) yields

$$b_{10}=\frac{(m_1+m_2)R_w^2(1-s_0)+J_w+\left(J_e\omega_{e0}-J_e\omega_{eT}-J_eh_0\tilde{t}\right)/\omega_{w0}}{(m_1+m_2)R_w^2} \tag{15}$$

Note that $\dot{\theta}_e$ is a slowly varying function when the opening angle is a constant, we have the value of ω_{e0} is almost equal to the value of ω_{eT}. Insertion of Equation (14) to b_{10} in Equation (15) leads to the following

$$b_{10}=\frac{\omega_{eT}}{\omega_{w0}}b_1 \tag{16}$$

where $b_1=\dfrac{\omega_{w0}}{\omega_{eT}}\dfrac{(m_1+m_2)R_w^2(1-s_0)+J_w}{(m_1+m_2)R_w^2}$

Taking into accounted with Equation (14), we have

$$\frac{\omega_{w0}}{\dot{x}+\dot{\theta}_e}=\frac{\omega_{w0}}{\dot{x}+\omega_{eT}+h_0\tilde{t}}=\omega_{w0}\left[\frac{1}{\dot{x}+\omega_{eT}}-\frac{h_0\tilde{t}}{\left(\dot{x}+\omega_{eT}+h_0\tilde{t}\right)\left(\dot{x}+\omega_{eT}\right)}\right]$$

By noting that the value of ω_{e0} is almost equal to the value of ω_{eT} and $0<h_0\square\omega_{eT}$, ignoring some terms in the above equation results in the equation of the following

form as

$$\frac{\omega_{w0}}{\dot{x}+\dot{\theta}_e}=\frac{\omega_{w0}}{\omega_{eT}}\frac{\omega_{eT}}{\dot{x}+\omega_{eT}} \tag{17}$$

Substituting Equation (16) and Equation (17) into Equation (12) yields a set of two first-order differential equations of the following form as

$$\begin{cases}\dfrac{dx}{dt}=y\\ \dfrac{dy}{dt}=-a_0x-a_1y+a_2e^{c_2b_1\frac{\omega_{eT}}{y+\omega_{eT}}}-a_3b_1\dfrac{\omega_{eT}}{y+\omega_{eT}}\end{cases} \tag{18}$$

As seen from Equation (18), the constant coefficients of rolling resistance have no effect on the shape of the trajectory of the dynamic system. To difficult values of them, the trajectory just shifts left or right.

3. THE EXISTENCE OF A LIMIT CIRCLE AND THE SELF-EXCITED VIBRATION

To a second-order ordinary differential equation as Equation (18), the followings proved that its trajectory is a limit circle based on Poincaré-Bendixson Annulus Theorem. According to the differential equation theories, a limit circle means the existence of the self-excited vibration in the vibration system.

3.1. The Trajectory

Theorem: The trajectory of Equation (18) is a limit circle, if the following two inequalities are satisfied:

$$\omega_{eT}>\frac{a_3b_1}{\sqrt{a_0}} \tag{19}$$

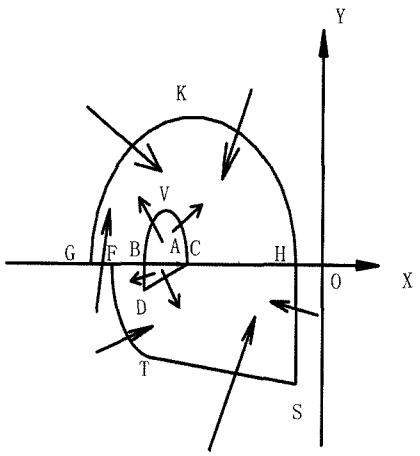

Figure 3. The interior boundary and the exterior boundary (for the existence).

$$a_3b_1-\sqrt{a_0}\omega_{eT}+a_2e^{\frac{\sqrt{a_0}\omega_{eT}c_2}{a_3}}-a_2e^{c_2b_1}>0 \tag{20}$$

Proof:

3.1.1. The interior boundary (See Figure 3)

By all appearances, Equation (18) has only one critical point A, and its coordinate is $\left(\frac{a_2}{a_0}e^{c_2b_1}-\frac{a_3}{a_0}b_1,0\right)$ (See Figure 3).The interior boundary is comprised of three curves. They are the following curves: an elliptic line BVC (ℓl_1), a line segment BD (ℓ_2) and a line segment CD (ℓ_3).

(1) Curve ℓ_1

The equation for ℓ_1 is given by

$$a_0\left[x-\left(x_A-\frac{\varepsilon_1}{\sqrt{a_0}+1}\right)\right]^2+y^2=\varepsilon_1^2 \tag{21}$$

where ε_1 is an undetermined positive constant. Then, the trajectory trend of Equation (18) with respected to curve ℓ_1 is given by

$$\left.\frac{d\ell_1}{dt}\right|_{eq18}=2y\left(a_3b_1-a_3b_1\frac{\omega_{eT}}{y+\omega_{eT}}-a_2e^{c_2b_1}+a_2e^{c_2b_1\omega_{eT}/(y+\omega_{eT})}+a_0\frac{\varepsilon_1}{\sqrt{a_0}+1}-a_1y\right) \tag{22}$$

Let y be the independent variable, and define the dependant variable $f_1(y)$ as follows

$$f_1(y)=a_3b_1-a_3b_1\frac{\omega_{eT}}{y+\omega_{eT}}-a_2e^{c_2b_1}+a_2e^{c_2b_1\frac{\omega_{eT}}{y+\omega_{eT}}}+a_0\frac{\varepsilon_1}{\sqrt{a_0}+1}-a_1y \tag{23}$$

Clearly, $f_1(y)$ is a continuous function at y=0, and $f_1(0)=a_0\frac{\varepsilon_1}{\sqrt{a_0}+1}>0$. Hence, there is a neighborhood $\hbar_1$ of y=0, such that $f_1(y)>0$, for $y\in\hbar_1$. Let $y_{1\max}$ be the maximum value of y in $\hbar_1$, and let $\varepsilon_1=y_{1\max}$, then, the coordinate of y for the line ℓ_1 is no larger than ε_1, and is no less than zero. Hence, we have

$$\left.\frac{d\ell_1}{dt}\right|_{eq18}\geq 0\ \left(\left.\frac{d\ell_1}{dt}\right|_{eq18}=0\ \text{if and only if}\ y=0\right)$$

(2) Curve ℓ_2

The equation for ℓ_2 can be easily written bellow

$$x=x_B \tag{24}$$

Then, the trajectory trend of Equation (18) with respected to curve ℓ_2 is given by

$$\left.\frac{d\ell_2}{dt}\right|_{eq18}=\dot{x}=y. \tag{25}$$

To ℓ_2, its coordinate of y is lower than zero. Hence, we have

$$\frac{d\ell_2}{dt_{eq18}} < 0.$$

(3) Curve ℓ_3

The equation for ℓ_3 is given by

$$y - \varepsilon_2(x - x_C) = 0 \tag{26}$$

where ε_2 is an undetermined positive constant. Then, the trajectory trend of Equation (18) with respected to curve ℓ_3 is given by

$$\frac{d\ell_3}{dt_{eq18}} = -(\varepsilon_2 + \frac{a_0}{\varepsilon_2} + a_1)y - a_0(x_A + \frac{\varepsilon_1}{\sqrt{a_0}} - \frac{\varepsilon_1}{\sqrt{a_0}+1}) + a_2 e^{c_2 b_1 \frac{\omega_{eT}}{y+\omega_{eT}}} - a_3 b_1 \frac{\omega_{eT}}{y+\omega_{eT}} \tag{27}$$

Let y be the independent variable, and define the dependant variable $f_2(y)$ as follows

$$f_2(y) = -(\varepsilon_2 + \frac{a_0}{\varepsilon_2} + a_1)y - a_0(x_A + \frac{\varepsilon_1}{\sqrt{a_0}} - \frac{\varepsilon_1}{\sqrt{a_0}+1}) + a_2 e^{c_2 b_1 \frac{\omega_{eT}}{y+\omega_{eT}}} - a_3 b_1 \frac{\omega_{eT}}{y+\omega_{eT}} \tag{28}$$

Clearly, $f_2(y)$ is a continuous function at y=0, and

$f_2(0) = -a_0(\frac{\varepsilon_1}{\sqrt{a_0}} - \frac{\varepsilon_1}{\sqrt{a_0}+1}) < 0$. Hence, there is a neighborhood $\hbar_2$ of y=0, such that $f_2(y)$<0, for $y \in \hbar_2$. Let y_{2min} be the minimum value of y in region $\hbar_2$, then, a curved line between Point D(x_B, y_{2min}) and Point C can be found as ℓ_3. To ℓ_3, its coordinate of y is smaller than zero, and is no larger than y_{2min}. Hence, the following inequality is satisfied

$$\frac{d\ell_3}{dt_{eq18}} < 0.$$

Consequently, a closed interior boundary including three line segments *BVC-CD-DB* is configurated. The only critical point A is accommodated in the region, which is bounded by the interior boundary.

3.1.2. The exterior boundary (See Figure 3)

The exterior boundary is composed of five curves. They are the followings: an elliptic curve FT(ℓ_4), an elliptic curve GKH(ℓ_5), a line segment HS(ℓ_6), a line segment FG(ℓ_7) and a line segment TS(ℓ_8).

(1) Curve ℓ_4

The equation for ℓ_4 is given by

$$a_0\left[x - (x_A - \frac{\varepsilon_4}{\sqrt{a_0(1+M)}})\right]^2 + y^2 = \varepsilon_4^2 \tag{29}$$

where $\varepsilon_4 = \omega_{eT} - \frac{a_3 b_1 (1+M)}{\sqrt{a_0}}$, and M is an undetermined positive constant. Then, the trajectory trend of Equation (18) with respected to curve ℓ_4 is given by

$$\frac{d\ell_4}{dt_{eq18}} = 2y\left(a_3 b_1 - a_3 b_1 \frac{\omega_{eT}}{y+\omega_{eT}} - a_2 e^{c_2 b_1} + a_2 e^{c_2 b_1 \frac{\omega_{eT}}{y+\omega_{eT}}} + a_0 \frac{\varepsilon_4}{\sqrt{a_0(1+M)}} - a_1 y\right) \tag{30}$$

If $\omega_{eT} > \frac{a_3 b_1}{\sqrt{a_0}}$ (Inequality (19)), then there is a neighborhood χ of y=0, such that $\frac{d\ell_4}{dt_{eq18}} < 0$, for $y \in \chi$.

Clearly, if the positive constant M is little enough (the less, the better), then $M \in \chi$. Hence, we have

$$\frac{d\ell_4}{dt_{eq18}} \le 0 \quad (\frac{d\ell_4}{dt_{eq18}} = 0 \text{ if and only if } y = 0).$$

(2) Curve ℓ_5

The equation for ℓ_5 is given by

$$a_0\left[x - (x_A + \frac{\varepsilon_5}{\sqrt{a_0(1+N)}})\right]^2 + y^2 = \varepsilon_5^2 \tag{31}$$

where ε_5 and N are undetermined positive constants, Then, the trajectory trend of Equation (18) with respected to curve ℓ_5 can be presented in terms of x, y, $\dot{x}$ and $\dot{y}$ as follows

$$\frac{d\ell_5}{dt_{eq18}} = 2a_0\left[x - (x_A + \frac{\varepsilon_5}{\sqrt{a_0(1+N)}})\right]\dot{x} + 2y\dot{y} \tag{32}$$

It is easy to prove the followings: To an arbitrary positive constant N, if $\varepsilon_5 > \frac{a_3 b_1 (1+N)}{\sqrt{a_0}} - \omega_{eT}$, then $\frac{d\ell_5}{dt_{eq18}} < 0$.

As shown in Figure 3, however, in order to assure $x_G < x_F$, the following inequality is required as

$$\frac{\varepsilon_5}{\sqrt{a_0}} > \varepsilon_4\left(\frac{1}{\sqrt{a_0}} + \frac{1}{\sqrt{a_0(1+M)}}\right) + \frac{\varepsilon_5}{\sqrt{a_0(1+N)}}$$

That is

$$\varepsilon_5 > \frac{\varepsilon_4\left(1+\frac{1}{1+M}\right)}{1-\frac{1}{1+N}}.$$

Therefore, Let $\varepsilon_5=\max\left(\frac{\varepsilon_4\left(1+\frac{1}{1+M}\right)}{1-\frac{1}{1+N}}, \frac{a_3b_1(1+N)}{\sqrt{a_0}}-\omega_{eT}\right)+1$

(where the result of function max(a,b) is the larger of a and b), then, to an arbitrary positive constant N, the following inequality is satisfied

$$\frac{d\ell_5}{dt_{eq18}} < 0 .$$

(3) Curve ℓ_6

The equation for ℓ_6 can be expressed below

$$x=x_H \tag{33}$$

Then, the trajectory trend of Equation (18) with respected to curve ℓ_6 is given by

$$\frac{d\ell_6}{dt_{eq18}} = \dot{x}=y . \tag{34}$$

The coordinate of y for ℓ_6 is less than zero. Hence, we have

$$\frac{d\ell_6}{dt_{eq18}} < 0 .$$

(4) Curve ℓ_7

The equation for ℓ_7 is given by

$$y=0 \tag{35}$$

Then, the trajectory trend of Equation (18) with respected to curve ℓ_7 is given by

$$\frac{d\ell_7}{dt_{eq18}} = \dot{y} = -a_0x - a_1.0 + a_2e^{c_2b_1\frac{\omega_{eT}}{0+\omega_{eT}}} - a_3b_1\frac{\omega_{eT}}{0+\omega_{eT}} \tag{36}$$

The coordinate of x for ℓ_7 changes in the region given below

$$x_F \geq x \geq x_G .$$

Note that (See Figure 3)

$$x_A > x_F ,$$

Therefore

$$x < x_A .$$

Hence, we have

$$\frac{d\ell_7}{dt_{eq18}} > -a_0x_A + a_2e^{c_2b_1} - a_3b_1 = 0.$$

(5) Curve ℓ_8

The equation for ℓ_8 is given by

$$y+\varepsilon_4+\varepsilon_6(x-x_T)=0 \tag{37}$$

where ℓ_6 is an undetermined positive constant $\omega_{w0} \geq \varepsilon_6$, and $x_T = x_A - \frac{\varepsilon_4}{\sqrt{a_0}(1+M)}$ (See Figure 3). Then, the trajectory trend of Equation (18) with respected to curve ℓ_8 is given by

$$\frac{d\ell_8}{dt_{eq18}} = (\varepsilon_6 + \frac{a_0}{\varepsilon_6} - a_1)y + a_0\frac{\varepsilon_4}{\varepsilon_6} + a_0\frac{\varepsilon_4}{\sqrt{a_0}(1+M)} + a_3b_1 - a_3b_1\frac{\omega_{eT}}{y+\omega_{eT}} + a_2e^{c_2b_1\frac{\omega_{eT}}{y+\omega_{eT}}} - a_2e^{c_2b_1} \tag{38}$$

In the line segment TS (see Figure 3), clearly

$$y > Y_S,$$

where $Y_s = -\varepsilon_4 - \varepsilon_6\left(x_H - x_T\right) =$

$$-\varepsilon_4 - \varepsilon_6\left[\varepsilon_5\left(\frac{1}{\sqrt{a_0}}+\frac{1}{\sqrt{a_0}(1+N)}\right)+\frac{\varepsilon_4}{\sqrt{a_0}(1+M)}\right].$$

It is clearly that there is at least a positive constant ε_6, such that $\varepsilon_6 - a_1 < 0$ and $Y_s > -\varepsilon_4(1+M)$. Hence, we have

$$\frac{d\ell_8}{dt_{eq18}} > a_3b_1 - a_3b_1\frac{\omega_{eT}}{y+\omega_{eT}} + a_2e^{c_2b_1\frac{\omega_{eT}}{y+\omega_{eT}}} - a_2e^{c_2b_1} - M\frac{a_0}{\varepsilon_6}\varepsilon_4$$

Note that $Y_S < y < -\varepsilon_4$, then

$$\frac{d\ell_8}{dt_{eq18}} > a_3b_1 - a_3b_1\frac{\omega_{eT}}{-(1+M)\varepsilon_4+\omega_{eT}} + a_2e^{c_2b_1\frac{\omega_{eT}}{-\varepsilon_4+\omega_{eT}}} - a_2e^{c_2b_1} - M\frac{a_0}{\varepsilon_6}\varepsilon_4 .$$

Letting $\varepsilon_6=\sqrt{M}$ and substituting $\varepsilon_4 = \omega_{eT} - \frac{a_3b_1(1+M)}{\sqrt{a_0}}$ into the above inequality lead

$$\frac{d\ell_8}{dt_{eq18}} > a_3b_1 - a_3b_1\frac{\omega_{eT}}{(1+M)\left[\frac{a_3b_1(1+M)}{\sqrt{a_0}}\right]-M\omega_{eT}} + a_2e^{c_2b_1\frac{\omega_{eT}}{\left[\frac{a_3b_1(1+M)}{\sqrt{a_0}}\right]}} - a_2e^{c_2b_1} - \sqrt{M}a_0\varepsilon_4 .$$

Similar to the proof of $\frac{d\ell_1}{dt_{eq18}} \geq 0$, it is easy to prove the followings: To the line segment *TS*, If Inequality (20) $(a_3 b_1 - \sqrt{a_0}\omega_{eT} + a_2 e^{\frac{\sqrt{a_0}\omega_{eT} c_2}{a_3}} - a_2 e^{c_2 b_1} > 0)$ is satisfied, then $\frac{d\ell_8}{dt_{eq18}} > 0$.

Now, a closed exterior boundary *GKH-HS-ST-TF-FG* is made, only if the positive constant *M* is small enough.

3.1.3. The existence of a limit circle and self-excited vibration

In the case that the interior boundary is intersected with the exterior boundary, reduction of the interior boundary should be made to certain dimensions until no intersection is found. Based on Poincaré-Bendixson Annulus Theorem, the trajectory of Equation (18) is a limit circle. We have thus proved the theorem, and the limit circle means the existence of the torsional self-excited vibration in the tractor's driveline.

However, the two conditions (Inequality (19) and Inequality (20)) are easy to be met, so there must exist self-excited vibration in the driveline.

3.2. The Amplitude of the Self-excited Vibration

In fact, the self-excited vibration in the driveline is not often found, although the present analysis implies existence of the nonlinear dynamic phenomenon. The reason is that the amplitude of the self-excited vibration is almost zero whenever the initial state satisfies the following inequality as

$$-a_1 - \frac{a_2 c_2 b_1}{\omega_{eT}} e^{c_2 b_1} + \frac{a_3 b_1}{\omega_{eT}} < 0 \tag{39}$$

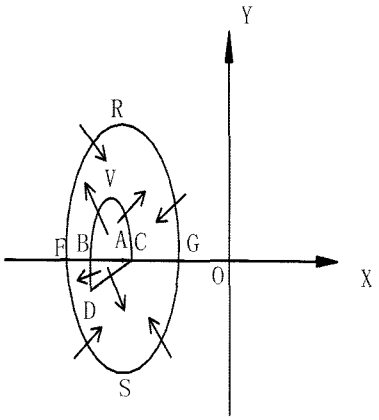

Figure 4. The interior boundary and exterior boundary (for the amplitude).

For a proof of the inference, new interior and exterior boundaries about the critical point A should be given again, as shown in Figure 4.

The interior boundary in Figure 4 is the same as the one in Figure 3 and the exterior boundary is an ellipse ℓ_9(*FRGSF*) in Figure 4. The equation for the closed elliptic curve ℓ_9 can be easily written below

$$a_0(x - x_A)^2 + y^2 = \varepsilon_9^2 \tag{40}$$

where ε_9 is an undetermined positive constant. Then, the trajectory trend of Equation (18) with respected to curve ℓ_9 is given by

$$\frac{d\ell_9}{dt_{eq18}} = 2y\left(a_3 b_1 - a_3 b_1 \frac{\omega_{eT}}{y + \omega_{eT}} - a_2 e^{c_2 b_1} + a_2 e^{c_2 b_1 \frac{\omega_{eT}}{y+\omega_{eT}}} - a_1 y\right) \tag{41}$$

Let y be the independent variable, and define the dependant variable $f_4(y)$ as follows

$$f_4(y) = a_3 b_1 - a_3 b_1 \frac{\omega_{eT}}{y + \omega_{eT}} - a_2 e^{c_2 b_1} + a_2 e^{c_2 b_1 \frac{\omega_{eT}}{y+\omega_{eT}}} - a_1 y \tag{42}$$

The function $f_4(y)$ is obviously a continuous and differential function at y=0. Obviously, the derivative of the function $f_4(y)$ can be obtained below

$$f_4'(y) = -a_2 \frac{c_2 b_1 \omega_{eT}}{(y + \omega_{eT})^2} e^{\frac{c_2 b_1 \omega_{eT}}{y+\omega_{eT}}} + a_3 b_1 \frac{\omega_{eT}}{(y + \omega_{eT})^2} - a_1 \tag{43}$$

Define the function $f_5(y)$ as follows

$$f_5(y) = -a_2 \frac{c_2 b_1 \omega_{eT}}{(y + \omega_{eT})^2} e^{\frac{c_2 b_1 \omega_{eT}}{y+\omega_{eT}}} + a_3 b_1 \frac{\omega_{eT}}{(y + \omega_{eT})^2} - a_1 \tag{44}$$

Clearly, the function $f_5(y)$ is a continuous function at y=0, and $f_5(0)<0$ when the inequality (39) is satisfied. Hence, there must exist a neighborhood $\hbar_4$ of y=0, in which $f_5(y)<0$. Suppose the maximum of y in region $\hbar_4$ is y_{4min}, and let $\varepsilon_9 = y_{4max}$, then, to ℓ_9, its coordinate of y is lower than y_{4max}, and is more than $-y_{4max}$. Distinguish with two cases: First, if $y>0$, then $f_4(y)<f_4(0)=0$. Thus, $yf_4(y)<0$. Hence, we have

$$\frac{d\ell_9}{dt_{eq18}} < 0$$

Second, if $y<0$, then $f_4(y)>f_4(0)=0$. Thus, $yf_4(y)<0$. Hence, the following inequality is also satisfied as

$$\frac{d\ell_9}{dt_{eq18}} < 0$$

Therefore, we have

$$\frac{d\ell_9}{dt_{eq18}} < 0$$

Again, if the interior boundary is intersected with the elliptic curve *FRGSF* of the exterior boundary, dimension of the interior boundary should be reduced to be less until no intersection is found. When the inequality in Equation (39) is satisfied, however, there is a limit circle in the region restrained between the interior and the exterior boundaries.

Because the y coordinate of the closed orbit (limit cycle) varies in the range from y_{4max} to $-y_{4max}$, the amplitude of the self-excited vibration is less than y_{4max}. Meanwhile, y_{4max} is the maximum of the region in the neighborhood of y=0, so that y_{4max} is almost zero. Accordingly, when the inequality (39) is satisfied, the amplitude of the self-excited torsional vibration is nearly equal to zero, either.

To most working modes of vehicles and tractor vehicles, the inequality (39) is satisfied. Therefore, the torsional self-excited vibration can't be found. However, there are some working modes which don't satisfy the inequality (39), such as high slip rate working mode. A tractor vehicle towing a very heavy trailer and a vehicle running on an rapid uphill road are examples of high slip rate, and the amplitude of the torsional self-excited vibration can be observed and tested.

4. EXPERIMENTAL RESULTS AND NUMERICAL SIMULATIONS

In order to test whether there is self-excited torsional vibration or not, SZG4032 type tractor made by a local vehicle manufacturer is employed for validation. On the other hand, a load carrier used to act as a trailer. Dynamic parameters of the tractor and the load carrier are presented in Table 1. The SZG4032 tractors are used in Chinese airports for towing cargo trailers. The load carrier can produce required resistance force to increase the traction of the tractor. The added resistance force is expressed by the parameter of f_2. The main instruments are shown in Figure 5, other experimental instruments include a DAQCard-6062E (made by NI), a SCXI1000 (made by NI) and accelerator sensors, etc. By those instruments, data including vertical accelerations of the front and rear axles, the longitudinal velocity of the tractor, the angular velocity of the driving wheel, the traction force and the slip rate are acquired. Though the real-time slip and tractive force, the adhesive- coefficient experimental curve is got, then ,the parameters of the adhesive- coefficient fitting curve are calculated, as shown in Table 1.

At first, the biggest initial slip which satisfies the inequality (39) is calculated as follows: Suppose the function $z(s_0)$ is given by

$$z = -a_1 - \frac{a_2 c_2 b_1}{\omega_{eT}} e^{c_2 b_1} + \frac{a_3 b_1}{\omega_{eT}} \tag{45}$$

Substituting the parameters into Equation (45) and drawing the relation of $z(s_0)$ and s_0 yield Figure 6 and

Table 1. the parameters of a tractor and trailer.

m_1 (kg)	m_2 (kg)	ω_{eT} (rad/s)
3480	2000	5.8
R_w (m)	J_e (kg m^2)	J_w (kg m^2)
0.36	960	40
K (N/rad)	C (N s/rad)	C_1
12000	80	0.8
C_2	C_3	
50	0.4	

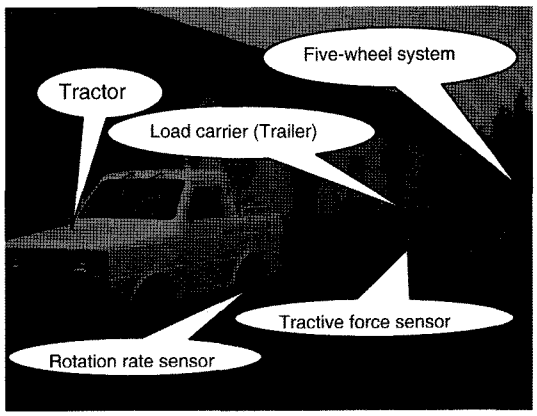

Figure 5. The sketch of the testing system.

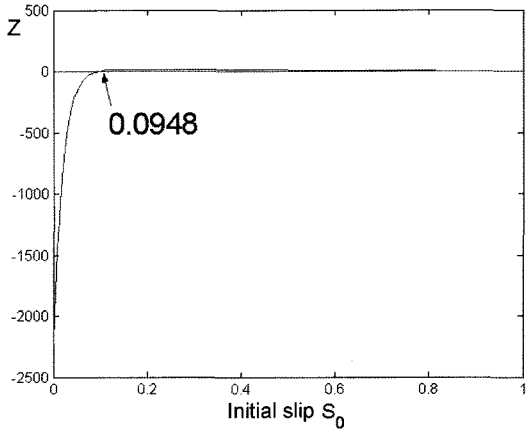

Figure 6. The relation of $z(s_0)$ and s_0.

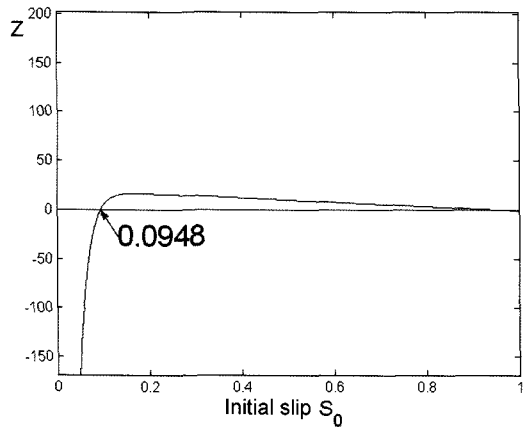

Figure 7. Partial enlarged.

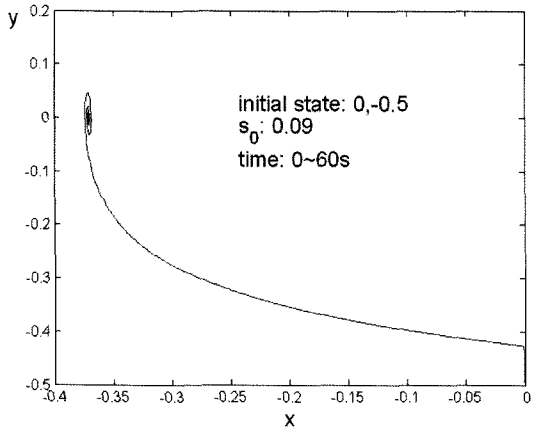

Figure 8. The general view of the trajectory (s_0=9%).

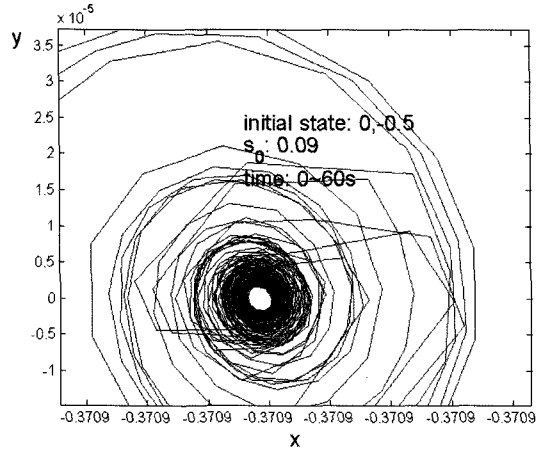

Figure 9. Tthe localized view.

Figure 7 Figure 6 and Figure 7 show the amplitude of torsional self-excited vibration is almost zero when the initial slip s_0 is less than 9.48%. Suppose the initial slip rate is 9%, the numerical solutions are shown in Figure 8

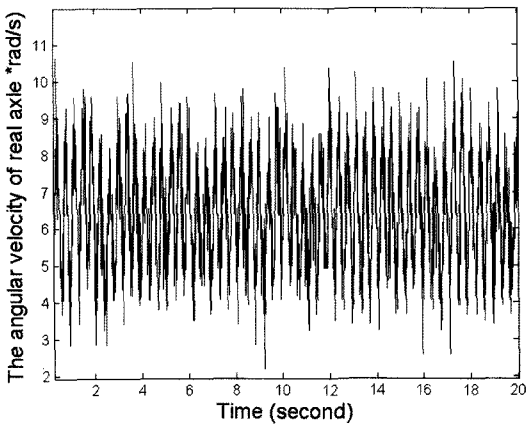

Figure 10. The experimental results of the velocity of rear axle.

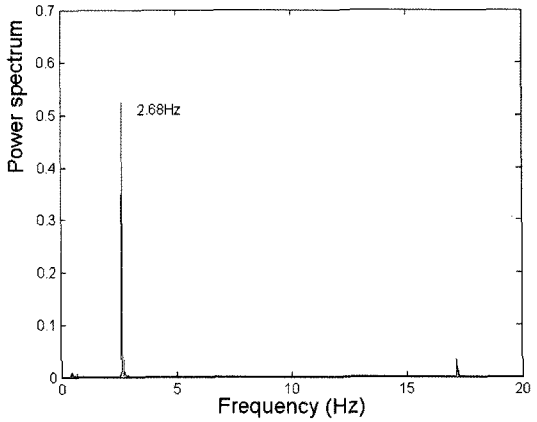

Figure 11. The frequency domain response (power spectrum).

and Figure 9. Torsional self-excited vibration does exist, but the amplitude is almost zero.

In the experiments, by increasing the resistance force of the load carrier, the initial slip of the tractor adds to be 39.5%. According to the above analysis, this initial slip does not satisfy Equation (39), the amplitude may be large. The experimental results are shown as Figure 10 and Figure 11.

The results of numerical simulations are shown as Figure 12 and Figure 13.

The frequency can be calculated by Average Method as follows: Let $x=A\cos\theta$, $\dot{x}=-Af_T\sin\theta$, and $\ddot{x}=-A_fT^2\cos\theta$, then, from Equation (18) we have

$$-Af_T{}^2\cos\theta + a_0A\cos\theta - a_1Af_T\sin\theta - a_2e^{c_2b_1\frac{1}{1-\frac{Af_T}{\omega_{w0}}\sin\theta}} + a_3b_1\frac{1}{1-\frac{Af_T}{\omega_{w0}}\sin\theta} = 0 \tag{46}$$

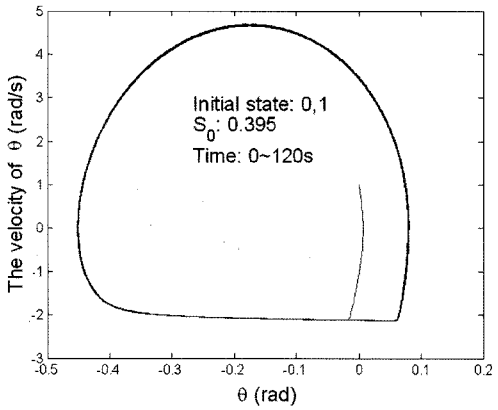

Figure 12. The trajectory of equation (18) (s_0=39.5%).

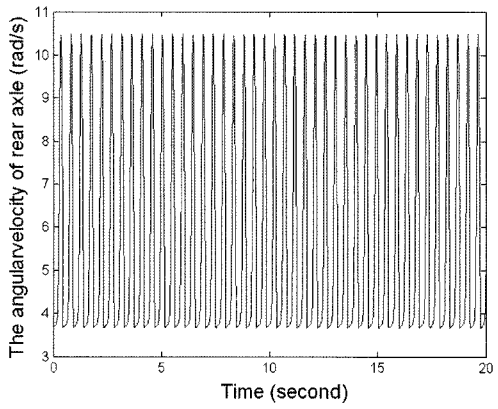

Figure 13. Simulation results of the velocity of rear axle.

Note that $\int_0^{2\pi} \frac{1}{1-r\sin\theta}\cos\theta d\theta = 0$ and

$\int_0^{2\pi} e^{c_2 b_1 \frac{1}{1-r\sin\theta}} \cos\theta d\theta = 0$ (where r is a constant),

Equation (46) multiplied with $\cos\theta d\theta$ and integration in $[0,2\pi]$ yield

$$f_1 = \sqrt{a_0} \tag{47}$$

Substituting the parameters into Equation (47) yields f_1=2.8H_z. The existence of self-excited torsional vibration in the tractor's driveline is demonstrated in case of different initial slips. It is also shown from the comparison of the frequency obtained by the present approximation and experiment that the two results are in fairly good agreement.

5. CONCLUSIONS

The existence of torsional self-excited vibration in wheeled tractor's driveline was proved by mathematical analysis. Two conditions which assure the existence of torsional self-excited vibration were put forward, and most of vehicle's working modes satisfy these conditions. At the same time, The third condition which assures the amplitude of the torsional self-excited vibration is almost zero was also put forward, and most vehicle's working modes satisfy the third condition. The tractor's working modes do not satisfy the third condition are few, such as towing a heavy trailer and running on the road whose slope is big. Numerical simulations and experiments are performed to show the existence of torsional self-excited vibration in wheeled tractor's driveline.

ACKNOWLEDGEMENT–This work is financially supported in parts by Chinese National High Technology Development (863) Program (Grant Number: 2001AA505000-114) and National Key Laboratory of Vibration, Shock and Noise Special Funding.

REFERENCES

Bailey, P. H., Reece, A. R. and Wills, B. M. D. (1962). A comparison between the performance of wheels when fitted to two wheel-testing machines and to a normal tractor. *J. Agricultural Engineering Research,* **1,** 61–63.

Christopher, S. Keeney and Shan, S. (1992). Prediction and control of heavy duty powertrain torsional vibration. *SAE Paper No.* 922481.

Couderc, J., Callenare, J., Hagopian, D. and Ferraris, G. (1998). Vehicle driveline dynamic behavior; experiment and simulation. *J. Sound and Vibration* **218, 1,** 133–157.

Farong, Z. and Parker, R. G. (2005). Non-linear dynamics of a one-way clutch in belt-pulley systems. *J. Sound and Vibration* **279, 1-2,** 285–308.

Ford, R. A. J. and Karam, H. (1991). Self-excited vibration of a semi-trailer rig. *Trans. Institution of Engineers, Australia: Mechanical Engineering*, **ME 16, 1,** 69–72.

Ge, J. M., Wang, Z. M. and Zheng, L. Z. (2003). Simulation of self-excited vibration on vehicle power train. *Trans. Chinese Society of Agricultural Machinery (in Chinese)* **34, 3,** 1–4.

Hwang, S. J., Chen, J S. Liu, L. and Ling, C. C. (2000). Modeling and simulation of a powertrain-vehicle system with automatic transmission. *Int. J. Vehicle Design* **23, 1,** 145–160.

Hwang, S. J., Joseph, L. Stout and Ling, C. C. (1998). Modeling and analysis of powertrain torsional response. *SAE Paper No.* 980276.

Jia, J. Z., Cheng, Y. S., Zheng, L. Z. and Shao, M. L. (1998). Experimental study on the self-excited vibration in vehicle powertrain. *Trans. Chinese Society of Agricultural Machinery (in Chinese)* **29, 4,** 1–5.

Jia, J. Z., Luo, X. W. and Shao, M. L. (1997a). Vehicle jumping phenomenon and self-excited vibration in vehicle transmission. *Zhongshan University Trans.*

Forum (in Chinese), **5,** 174–178.

Jia, J. Z., Wang, D. F. and Wang, Z. Z. (1997b). Research on the self-excited vibration in wheeled vehicle powertrain (part 4): Analysis of factors influencing vehicle stability and measures to control the self-excited vibration. *Trans. Chinese Society of Agricultural Engineering (in Chinese)* **13, 1,** 45–50.

Jia, J. Z., Zheng, L. Z. and Cheng, Y. S. (1996). Research on the self-excited vibration in wheeled vehicle powertrain (2): Analysis of energy feedback and control system, *Trans. Chinese Society of Agricultural Engineering (in Chinese)* **12, 4,** 43–47.

Olson, B. J., Shaw, S. W. and Stépán, G. (2000). Dynamics of vehicle traction. *Vehicle System Dynamics* **40, 6,** 377–399.

Wang, D. F. (2000). Stability analysis for self-excited torsional vibration of vehicle driveline. *Int. J. Vehicle Design* **24, 2,** 211–223.

Zheng, L. Z., Jia, J. Z. and Cheng, Y. S. (1996). Research on the self-excited vibration in wheeled vehicle powertrain (1): Mechanism analysis of self-excited vibration. *Trans. Chinese Society of Agricultural Engineering (in Chinese)* **12, 4,** 37–42.

Zheng, L. Z., Liu, M. S. and Zhang, Y. K. (2001). The mechanism of the self-excited torsional vibration in transmission system. *Automotive Engineering (in Chinese)* **23, 6,** 377–399.

Zheng, L. Z., Zhang, Y. K., Li, J. M. and Ge, J. M. (1997). Research on the self-excited vibration in wheeled vehicle powertrain (3): Stability analysis of the self-excited vibration system. *Trans. Chinese Society of Agricultural Engineering (in Chinese)* **13, 1,** 39–44.